# ENERGY-RESOLVED PULSE PROFILE VARIABILITY OF THE ACCRETING X-RAY PULSAR HER X-1 USING SWIFT/XRT OBSERVATIONS

**[1]Nikita Solanki, [*]Dr. Yogita Shrimali**
[1]Research Scholar, [*]HOD Assistant Professor
[1] J.R.N. Rajasthan Vidyapeeth (Deemed to be) University, Udaipur
[*]Department of Physics, J.R.N. Rajasthan Vidyapeeth (Deemed to be) University, Udaipur

***Abstract-***
The pulse profile and energy resolved lifetime of the long lived intermediate mass X-ray binary and accreting pulsar Hercules X-1 (Her X-1) are studied in great detail. The temporal behaviour of the system is studied on short time scales using a multi-epoch archival observations from the X-ray Telescope ( Swift/XRT) photon counting (PC) mode and on a longer time scales with the windowed timing (WT) mode. The light images (after background subtraction of images taken) reveal clearly distinct modulations which correspond to the magnetic precession modulations of 35 days with the orbital modulations. Epoch folding (efsearch and efold) is used to filter to a high signal to noise (SNR) X-ray pulse profile and is used to accurately measure spin periods. Furthermore, pulse profiles from the preprocessed disks and accreation column in different energy bands [soft (0.2–2 keV) and hard (2–10 keV)] show different pulse shapes, which suggest energy-dependent changes in the pulse shape due to the complex beaming geometries, the interaction and absorption of the photons in the preprocessed disks and accreation column. Deeper considerate of the radiative processes and accretion physics of strongly magnetized neutron star systems is made possible by these discoveries.
**Key words:** stars: neutron — pulsars: individual: Her X-1 — X-rays: binaries — Accretion, accretion disks.

## 1. INTRODUCTION

One of the brightest and most researched X-ray binaries is her X-1 (Fürst, F., et .al 2013). Hercules X-1 is a persistent accreting pulsar discovered as one of the primary X-ray sources by the Uhuru satellite in 1972 and ever since it is one of the most thoroughly-studied X-ray pulsars. The basic phenomenological picture of Her X-1 was established soon after its discovery: a close binary system consisting of an accreting magnetized neutron star with a 1.24 s spin period (D. Klochkov et al 2009). We used established protocols and the most recent calibration files available to examine the Swift /XRT data obtained in both photon counting mode (PC) and window timing mode (WT) (C. Ferrigno et al. 2011). The X-ray pulsations have been modeled as emission from an accretion column geometry that has been altered by light bending in the gravity of the neutron star (Denis Leahy et al. 2020). In order to enable disk geometry to change from the antisymmetric to asymmetric, we added a higher harmonic term to the azimuthal purpose of suggested warped-disk model. This adjustment can explain the phase shift that was noticed. Interestingly, the phase shift was accompanied by a drop in hard X-ray flux, which is probably comparable to the anomalous low state seen in Her X-1, which is thought to be caused by fluctuations in disk structure obscuring the X-ray emission area (Chou, Y. 2026). Fundamental insights into the physics of strong gravitational forces, high magnetic fields, and extreme plasma dynamics may be gained from the study of accreting X-ray binary systems. X-ray pulsars, both transient and persistent, are special natural laboratories. These systems usually consist of a highly magnetic neutron star that uses stellar wind or Roche-lobe overflow to accumulate materials from a stellar partner. On November 20, 2004, the Swift satellite was launched. Three co-aligned instruments are carried by Swift: the wide-field coded aperture mask The Ultraviolet/Optical Telescope (UVOT), the narrow field (23.6 × 23.6 arcmin2) grazing incidence Wolter-1 X-Ray Telescope (XRT; 0.2–10 keV), and the Burst Alert Telescope (BAT; 15–150 keV). We used PSR J1846-0258 data collected by XRT from routine monitoring observations starting on July 25, 2011. We only used the Windowed-Timing (WT) mode, which has a temporal resolution of 1.7675 ms and is adequately sufficient for pulse timing studies of PSR J1846−0258, out of the XRT's multiple operating modes (Kuiper, L., et al. 2018). It is a very strong magnetic field, as well as it attracts the incoming material towards magnetic poles, in which the potential energy of the material under the influence of gravity is converted to high energy x-ray radiation. Examining the spectral as well as temporal behavior of these systems facilitates the deciphering of the complex connections between radiative transmission, shock creation, and accretion geometry near the neutron star surface. Recent observational data from space-borne observatories have allowed astronomers to study short-term variability and pulse profile dynamics with previously unprecedented accuracy, improving our understanding of neutron star interiors and accretion mechanics.

## 2. ABOUT THE SOURCE

Hercules X-1 (Her X-1) is a classic accreting X-ray pulsar as well as the most researched intermediate-mass X-ray binaries (IMXRBs). The Uhuru spacecraft discovered the system in 1971. It is made up of an A/F-type companion star, HZ Herculis, and a revolving neutron star with orbital time of about 1.7 days. Her X-1 exhibits a number of unique periodicities, such as a prominent 35-day long-term intensity cycle with high-state ("Main-State" and "Short-State"), low-state, and anomalous low-state intervals; regular binary eclipses lasting roughly 0.2 days; and a fast spin period of roughly 1.24 seconds related with the neutron star rotation. Precession or tilting of a twisted accretion disk that periodically obscures the producing neutron star poles moreover the central X-ray source is often thought to be answerable for 35-day cycle. Her X-1 spectra also frequently exhibit complex absorption components and conspicuous cyclotron resonance scattering features (CRSFs), which makes it a perfect option for examining energy-dependent pulse profile fluctuations and absorption dynamics. Accretion disk precession, which causes varying obscuration of the X-ray generating areas on the neutron star's surface, is assumed to be the cause of this flux modulation. Her X-1 is noteworthy because to its unique spectrum characteristics in addition to its timing aspects. A soft blackbody, a power law, a Fe Kα line, exponential decay, and—most importantly—a cyclotron line at 40 keV are all seen in the broadband X-ray spectrum of Her X-1 in its main-on state (Xiao, G. C 2024). We have examined the system's spectrum features at various orbital phases in order to learn more about its nature. Our findings can shed some light on systems with abrupt off-states in X-ray intensity. Her X-1 and 4U 1626−67, which have low-mass partners, have demonstrated pulse frequency results that are in line with noise levels of 10−21 to 10−18 Hz s−2. Thus, torque noise fluctuation of the source can also be linked to residuals of quadratic fit (Şahiner, Ş., et al. 2013). We examine how LMC X-4's superorbital phase has evolved (Chou, Y. 2026). It was discovered that the pulse patterns in both observations had a double-peaked structure and only slightly depended on energy (Coley, J. B., et al .2019). According to estimates, Her X-1 is around 7 kpc away. Her X-1 is a brilliant and persistent source with reporting regularly of some interesting changing properties. Its period of rotation is 1.24 s and it has eclipsed every 1.7 d (Zhao, Q. C., et al. 2024).

## 3. OBSERVATIONS & DATA REDUCTION

This is info associated with the reduction and acquisition to the target data set. The X-ray data used for this study were obtained with the Swift X-ray Telescope (XRT) which is able of high spatial resolution imaging as well as sensitive X-ray spectroscopy. Data cleaning and filtering were done in HEASoft environment using the data cleaning and filtering criteria normally used in HEASoft and the Xselect software. Events in poor time intervals (PTL), e.g. Earth-limb, SAA (South Atlantic Anomaly) events and strong background flares were removed using Good Time Intervals (GTIs). The photons which have come from the target object were gathered within circular area that has been centered on the target coordinates and the background photons from the vicinity of the source (from the source-free sky regions) were taken into consideration rationally. C-statistic in XSPEC, distributed within HEASoft v6.3 (Nasa High Energy Astrophysics Science Archive Research Center (Heasarc) 2014) (Jayasurya, K. M., et al 2026). It is believed that the luminosity dependency is caused by varying accretion rates, which shift the line-forming region in the accretion column to higher or lower altitudes above the neutron star surface, leading to varying magnetic field strengths (Fuerst, F., et al 2013). The standard software (FTOOLS1 v6.29b), calibration (CALDB2 20210915), and techniques were used to process and evaluate all Swift data consistently. The task xrtpipeline (v0.13.6) was used to process and filter the Swift/XRT data (Ferrigno, C., et al 2022). Photons can undergo substantial energy shifts within the Doppler core of the cyclotron line due to resonant scattering by hot electrons (Salganik, A., et al. 2023). The photon counting data mode was used for all observations. Using the level-1 raw XRT event files, we started our study (Pasham, D. R., et al. 2013). We would like to encourage observers and model builders to keep gathering more observational data and gaining a better understanding of the physics underlying the many features of Her X-1 and other similar objects (Staubert, R., et al. 2014).

## OBSERVATION TABLES

**Table 1** The complete log of observations extracted from the HEASARC Swift/RXTE archive utilized in this work. The table details the observation identification numbers (ObsIDs), pointing coordinates (Right Ascension and Declination), start timestamps, processing dates, and effective exposure times across the XRT.

| S.No. | Obsid | RA | Dec | Start Time | Proc Date | XRT Exp [s] | UVOT Exp [s] | BAT Exp [s] | Arch Date |
|---|---|---|---|---|---|---|---|---|---|
| 1. | 00081452005 | 16 57 35.62 | +35 20 10.1 | 2016-08-20 04:46:58 | 2016-08-30 | 4780.95 | 4773.06 | 4796.00 | 2016-08-31 |
| 2 | 00081452004 | 16 57 36.06 | +35 19 20.4 | 2016-08-19 08:03:58 | 2016-08-29 | 2877.15 | 2865.21 | 2896.00 | 2016-08-30 |

| | | | | | | | | | |
|---|---|---|---|---|---|---|---|---|---|
| 3 | 00081452008 | 16 57 36.78 | +35 20 17.7 | 2017-08-06 01:43:57 | 2017-08-16 | 2129.11 | 2120.08 | 2134.00 | 2017-08-17 |
| 4 | 00089762001 | 16 57 34.27 | +35 20 00.4 | 2023-08-14 23:58:57 | 2023-08-25 | 2113.86 | 2218.90 | 2234.00 | 2023-08-25 |
| 5 | 00080177001 | 16 57 34.82 | +35 20 52.5 | 2012-09-19 17:51:59 | 2017-05-08 | 2107.95 | 2064.58 | 2114.00 | 2012-09-30 |
| 6 | 00081452001 | 16 57 37.72 | +35 20 00.0 | 2015-08-03 17:02:57 | 2015-08-13 | 2073.07 | 2065.84 | 2081.00 | 2015-08-14 |
| 7 | 00088111001 | 16 57 38.64 | +35 19 00.6 | 2017-08-05 12:52:57 | 2017-08-15 | 2073.03 | 2065.37 | 2080.00 | 2017-08-16 |
| 8 | 00081452006 | 16 57 32.11 | +35 20 16.9 | 2017-08-05 17:51:57 | 2017-08-15 | 1929.08 | 1922.88 | 1939.00 | 2017-08-16 |
| 9 | 00088781001 | 16 57 42.77 | +35 19 34.0 | 2018-07-14 03:36:57 | 2018-07-24 | 1908.20 | 1898.51 | 1908.00 | 2018-07-25 |
| 10 | 00081452007 | 16 57 33.94 | +35 20 03.9 | 2017-08-06 00:05:56 | 2017-08-16 | 1863.91 | 1855.73 | 1871.00 | 2017-08-17 |
| 11 | 00081452002 | 16 57 32.90 | +35 21 25.0 | 2015-08-09 00:26:58 | 2015-08-19 | 1856.87 | 1856.30 | 1871.00 | 2015-08-20 |
| 12 | 00089023002 | 16 57 53.87 | +35 19 44.1 | 2020-03-12 19:12:35 | 2020-03-22 | 1854.55 | 1830.53 | 1700.00 | 2020-03-23 |
| 13 | 00088781002 | 16 57 42.80 | +35 15 44.9 | 2019-06-23 17:36:35 | 2019-07-03 | 1808.07 | 1798.43 | 1813.00 | 2019-07-04 |

**Table 2** Log of observations extracted from the HEASARC Swift archive analyzed in this work, detailing the observation IDs, coordinates, start times, processing dates, and instrumental exposure times.

| S.No. | ObsID | RA | Dec | Start Time | Proc Date | XRT Exp[s] | UVOT Exo[s] | BAT Exo[s] | Archive Date |
|---|---|---|---|---|---|---|---|---|---|
| 1 | 03400064001 | 16 57 49.26 | +35 18 20.8 | 2025-06-16 10:30:57 | 2025-06-26 | 1664.12300 | 1662.30600 | 1670.00 | 2025-06-27 |
| 2 | 03400064002 | 16 57 35.81 | +35 19 21.0 | 2025-09-27 02:07:56 | 2025-10-07 | 1610.27400 | 1610.24400 | 1630.00 | 2025-10-08 |
| 3 | 03400015001 | 16 57 56.66 | +35 21 59.4 | 2025-01-30 01:33:12 | 2025-02-09 | 1788.8920 | 1779.643001 | 1795.00 | 1610.24400 |

## 4. TIMING AND ENERGY-RESOLVED PULSE PROFILE ANALYSIS

### 4.1 LIGHT CURVE GENERATION AND TEMPORAL VARIABILITY (LCURVE)

The lcurve tool was used to create background-subtracted light curves at different temporal resolutions to examine the lasting and short-term flux evolution. These are the normal modulations in intensity that are contained in the light curves, as well as the transitions between the bright and dark states of the source, and variations in intensity due to the orbit. The amount of inherent red noise and flare activity throughout the observation epochs is quantified using statistical studies of these light curves.

Figure 1 illustrates the temporal analysis of the Her X-1 utilizing data from ObsID 03400064001. The light curve shown here illustrates the intensity of the source, and is the most important data for setting up the timing baseline for the observation epoch. Changes and fluctuations in the count rate indicate the usual accretion process in this system.

Figure 2 shows the results of ObsID 03400064002. The sequence of observations was of great importance and applied to monitor the behaviour of the source over a long period of time. The provided ID may help to keep track of the stability of X-ray emission moreover to measure some key variations in X-ray brightness, potentially useful for characterisation of the immediate environment of the neutron star.

These are the data which come from the X-ray monitoring of Her X-1 (the third figure). The high and low state of the source can be measured or, when using the light curve, periodic eclipse of source due to the shadowing of the bigger companion. This data is also needed to ascertain that our chosen set of Observation IDs 03400015001 is not at bad phases of the binary orbit, and to make sure that the pulse profiling and timing analysis is not biased from occultation.

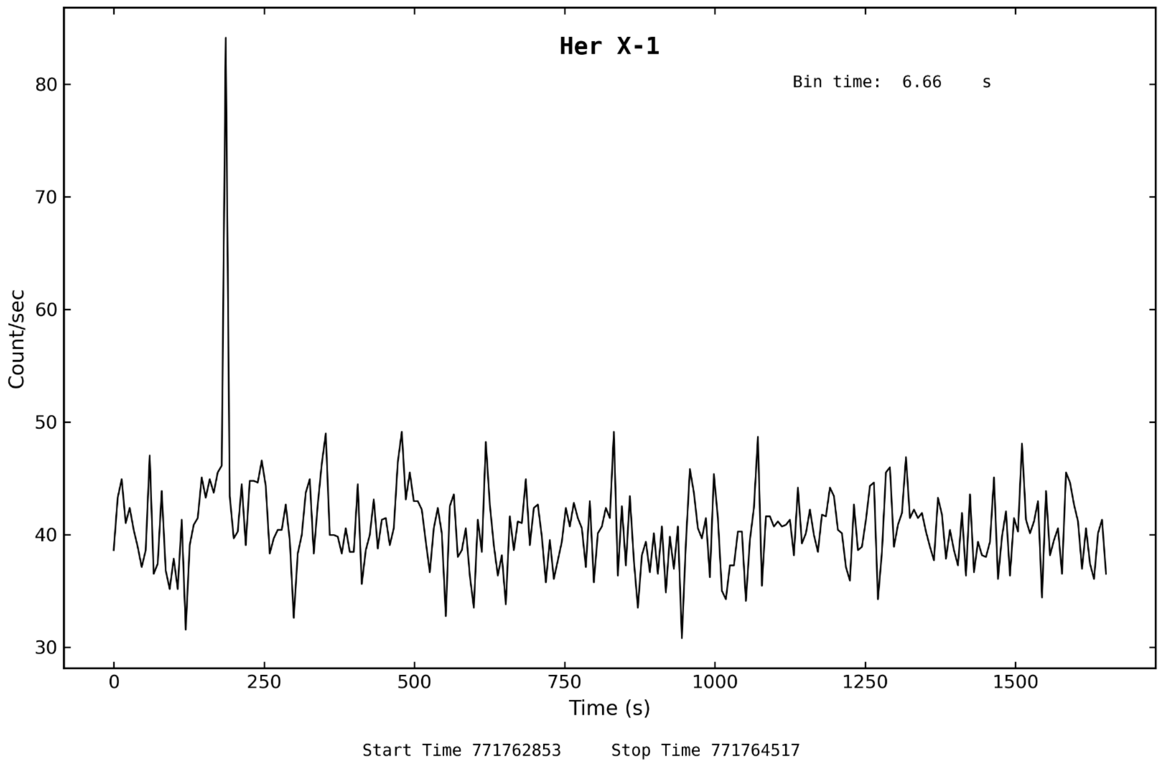


**Figure 1**: Light curve of Her X-1 showing count rate variations with time (bin time: 6.66 s) along with the observation start and stop times.

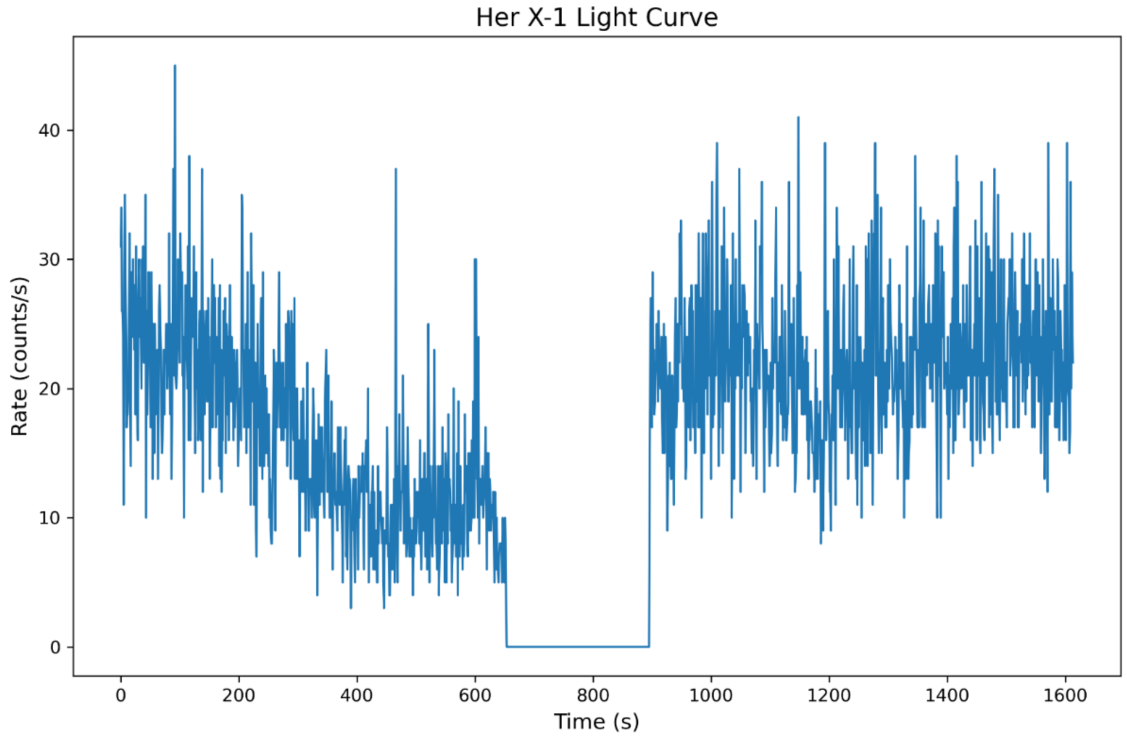


**Figure 2**: Light curve of Her X-1 illustrating (counts/s) count rate as function of time (s), highlighting variability and data gaps/state transitions.

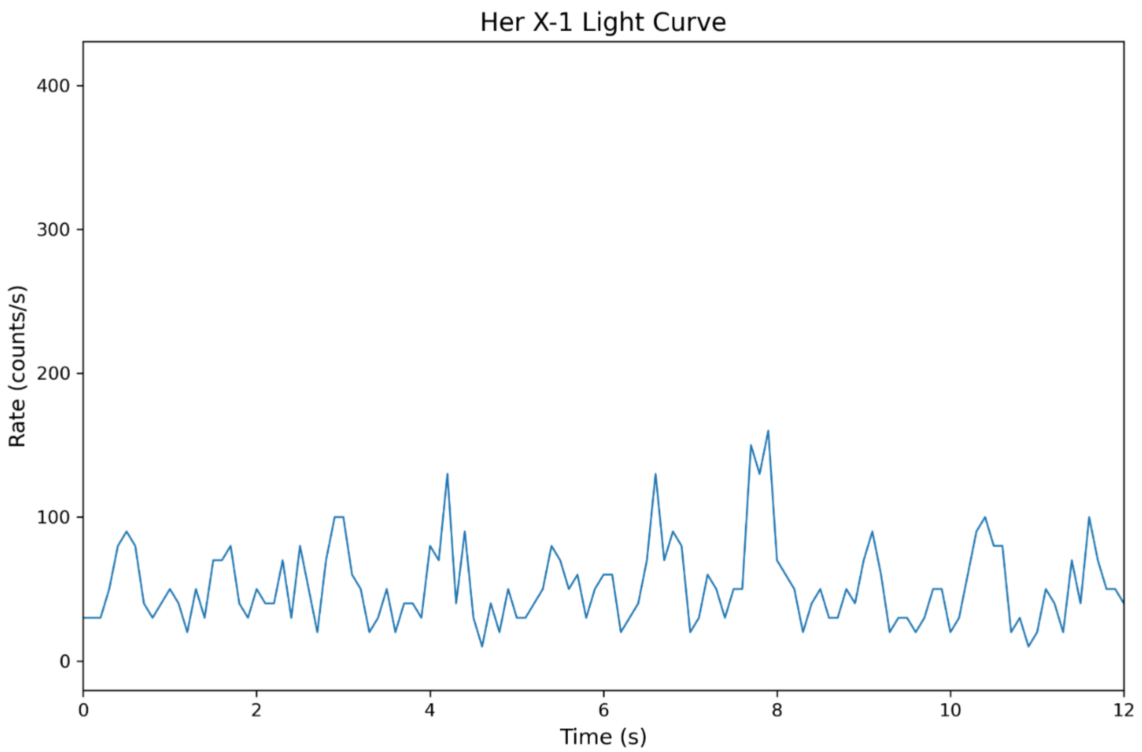


**Figure 3**: Light curve of Her X-1 plotted over a shorter time scale (0 to 12 s) displaying high-resolution count rate fluctuations.

**4.2 POWER DENSITY SPECTRA ANALYSIS (POWSPEC)**

We conducted a thorough spectrum study of NGC 3583 X-1 in XSPEC across two epochs using combination XMM-Newton + NuSTAR data from 2024 and XMM-Newton data from 2022 (Jayasurya, K. M.,2026). By using the Powspec task to compute Power Density Spectra (PDS), the source's quick temporal variability was investigated. The root-mean-square (rms) fractional variability over various frequency bands is assessed by the PDS profiles. We shed light on the noise processes originating inside the inner accretion disk and magnetospheric boundary layer by identifying distinctive frequencies, broad-band noise components, and upper limits on quasi-periodic oscillations (QPOs) by analysis of the power spectra. The measured Ecyc's linear dependency on X-ray flux (or brightness) is unmistakably confirmed by spectral analysis. The correlation's quantitative value, which has a slope of around 0.67 keV ASM-counts–1 s–1, is also replicated (Xiao, G. C 2024). Based on comparing the line centroids of the WT and PC Cas A spectra and using the XMM-RGS model to match the XRT/WT spectra of the SNR E0102-723 using the gain command inside Xspec, we calculated the systematic offset to be 17.6 eV (O. Godet et al. 2009).

The power density spectra are plotted for the two different observations of Her X-1 shown in Figures 4 and 5. For an intrinsic noise parameter analysis and for the study of rapid temporal evolution on a wide frequency range, plots such as shown herein are of special significance and are plotted for a typical plot duration of the main sensor of 0.05 seconds.

The power spectrum of the Her X-1 got from observation ID 03400015001 is shown in Figure 6. The power is mapped against frequency in this spectrum representation via Leahy normalization, which makes it possible to identify periodic signals and distinctive noise components present in the X-ray photon arrival times.

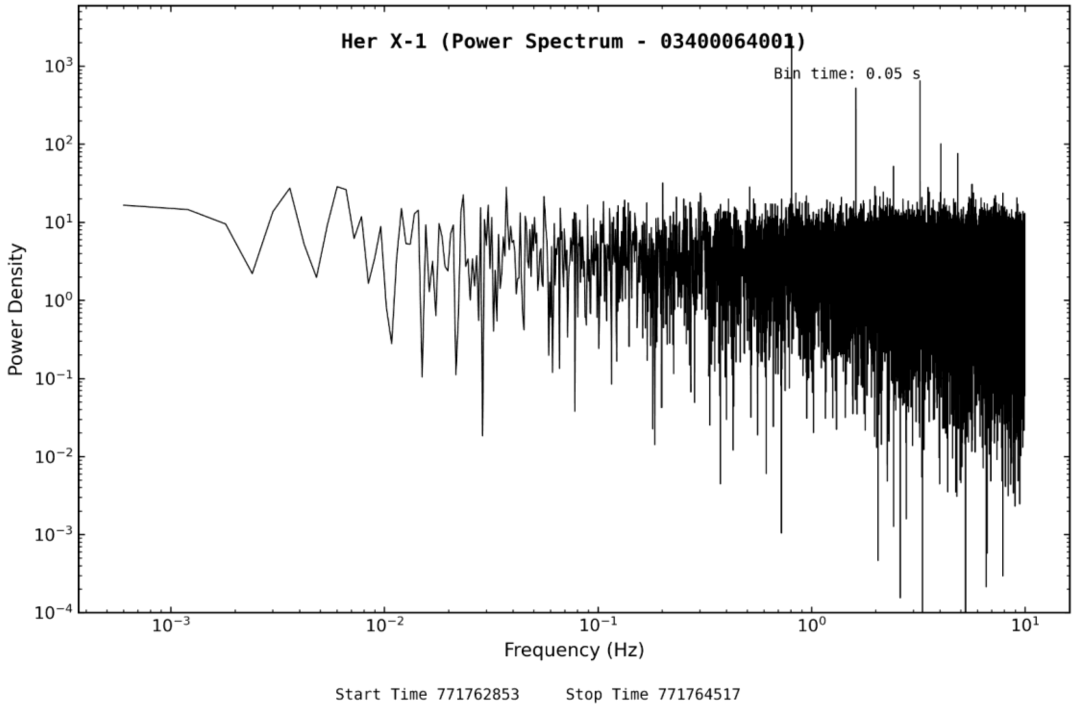


**Figure 4** A power spectrum analysis of the observations with Observation # 03400064001 was used to determine the power spectrum of the Her X-1.

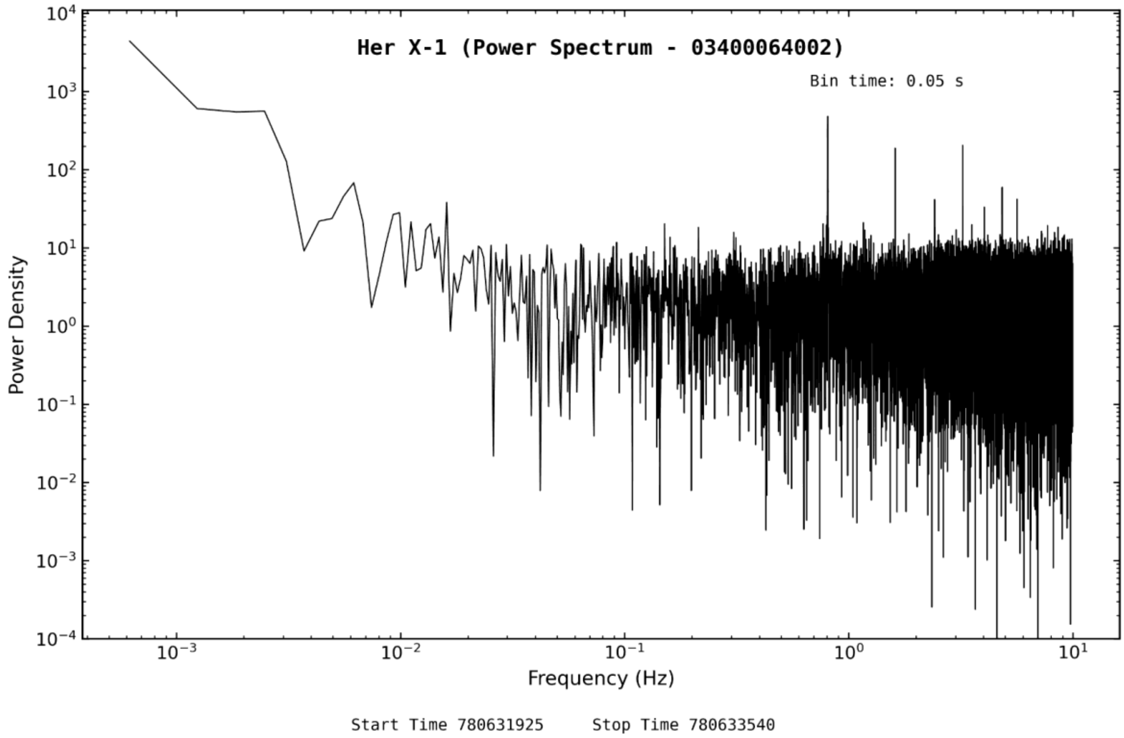


**Figure 5** In this case the power spectrum of Her X-1 is from Observation # 03400064002.

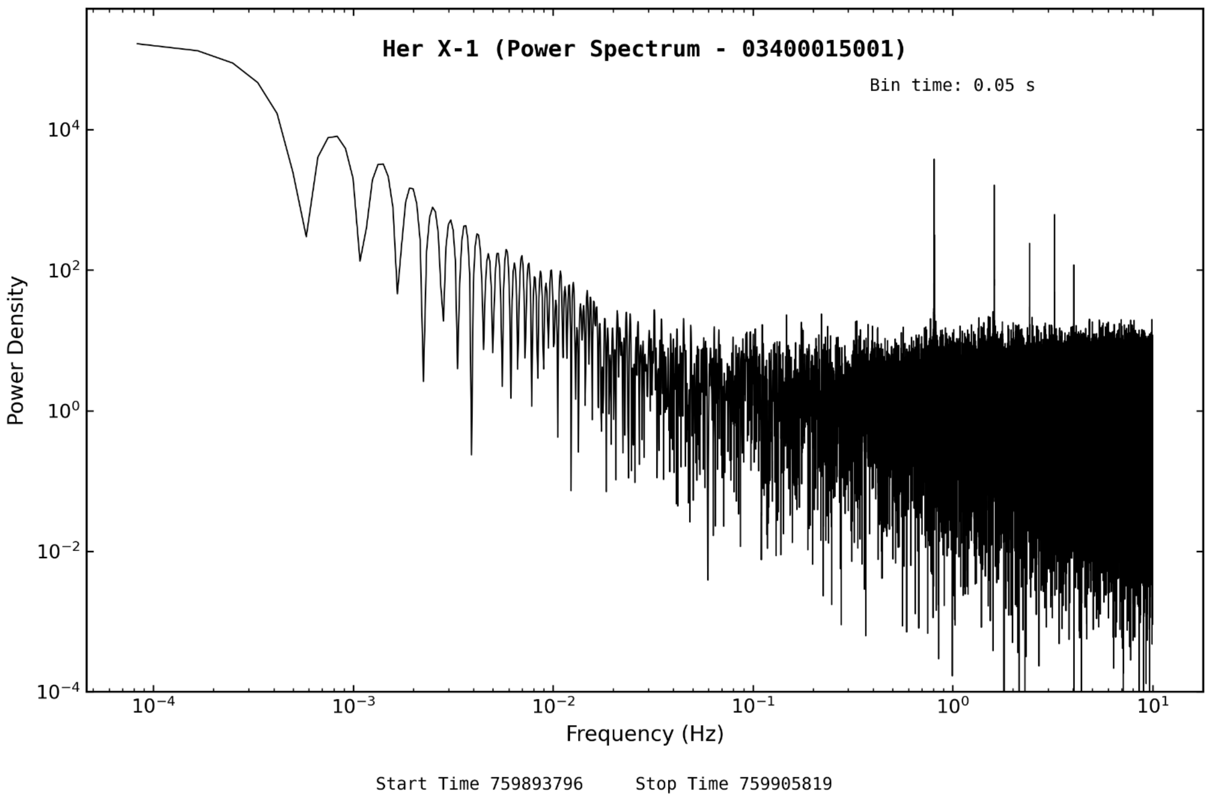


**Figure 6** The power spectrum of the observation #03400015001 of Her X-1 was obtained.

### 4.3 PERIOD DETERMINATION AND PULSATION SEARCH (EFSEARCH)

The efsearch tool was used to use period-search algorithms in order to exactly identify neutron star's spin period throughout the observation epoch. We created chi-squared (\chi^2) maximization curves by using epoch folding methods over a narrow grid of trial periods encompassing the predicted spin frequency. This thorough search corrects for any local Doppler shifts caused by the binary orbit and determines the pulse period with high statistical certainty.

We plot the luminosity of the two disk components and the total intrinsic luminosity as a function of superorbital phase and compare them to the average total luminosity observed from the Swift/XRT monitoring (Brightman, M., et al. 2022). The reduced chi-squared value ($\chi$ 2 red) and the associated degrees of freedom are reported for each fit (Ferrigno, C., et al. 2023).

Figure 7 presents the epoch folding analysis used to regulate the precise pulse time of Her X-1. By evaluating the chi-squared distribution against the period offset, the best-fit period and associated resolution are successfully extracted with high statistical certainty for the respective observation IDs. Best period is 1.237076794658 sec.

Figure 8 presents the epoch folding analysis used to control the precise pulse time of Her X-1. By evaluating the chi-squared distribution against the period offset, the best-fit period and associated resolution are successfully extracted with high statistical certainty for the respective observation IDs. Best period is 1.238420701169 sec.

The period search analysis for Her X-1 utilizing observation ID 03400015001 is presented in figure 9. The chi-squared variation against the period offset highlights the optimization process, yielding a robust best-fit pulse period of approximately 1.236 s with high statistical significanant.

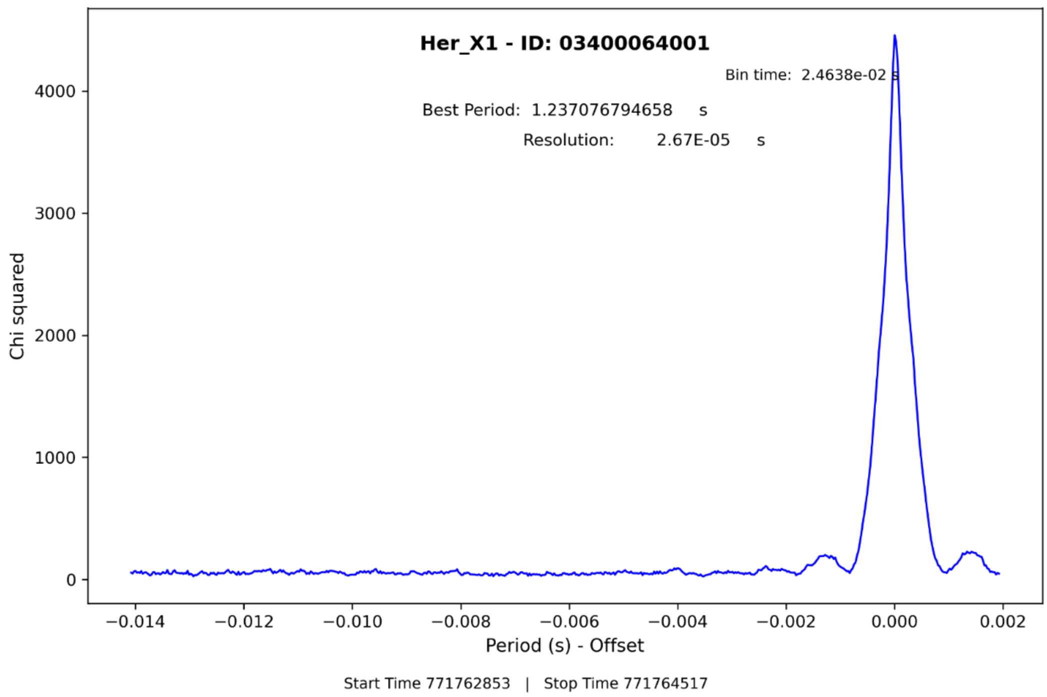


**Figure 7:** Chi-squared Period Search
The results from an efsearch analysis. The maximum value of \chi^2 corresponds to the maximum; the expected fit for the spin period of the pulsar.

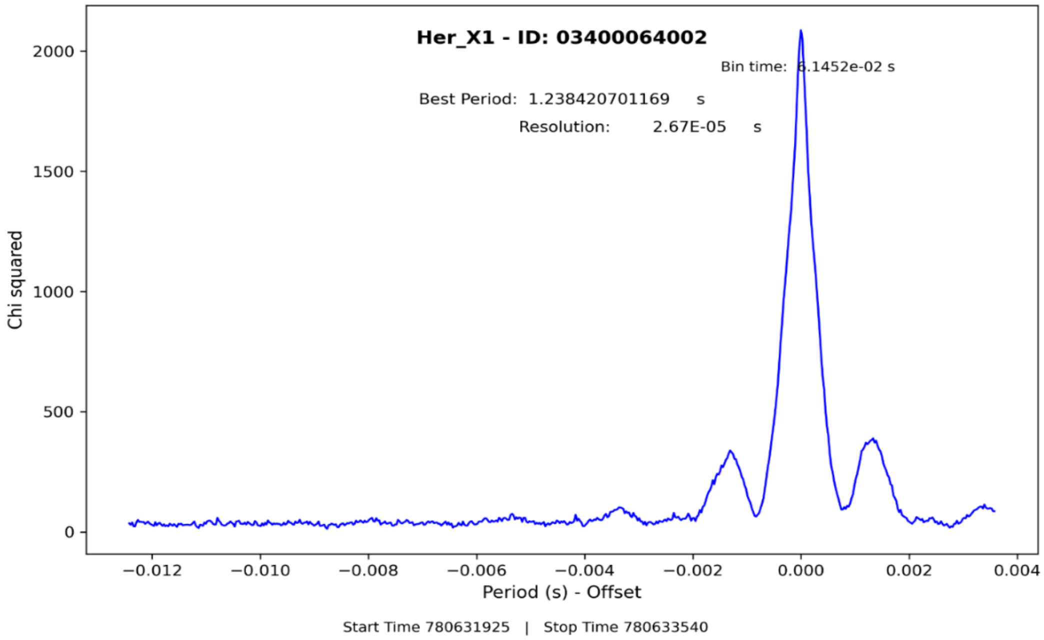


**Figure 8:** Chi-squared Period Search
Result obtained from the efsearch analysis. The best fit spin period of the pulsar is given by the maximum \chi^2 peak. Best Period: is 1.238420701169

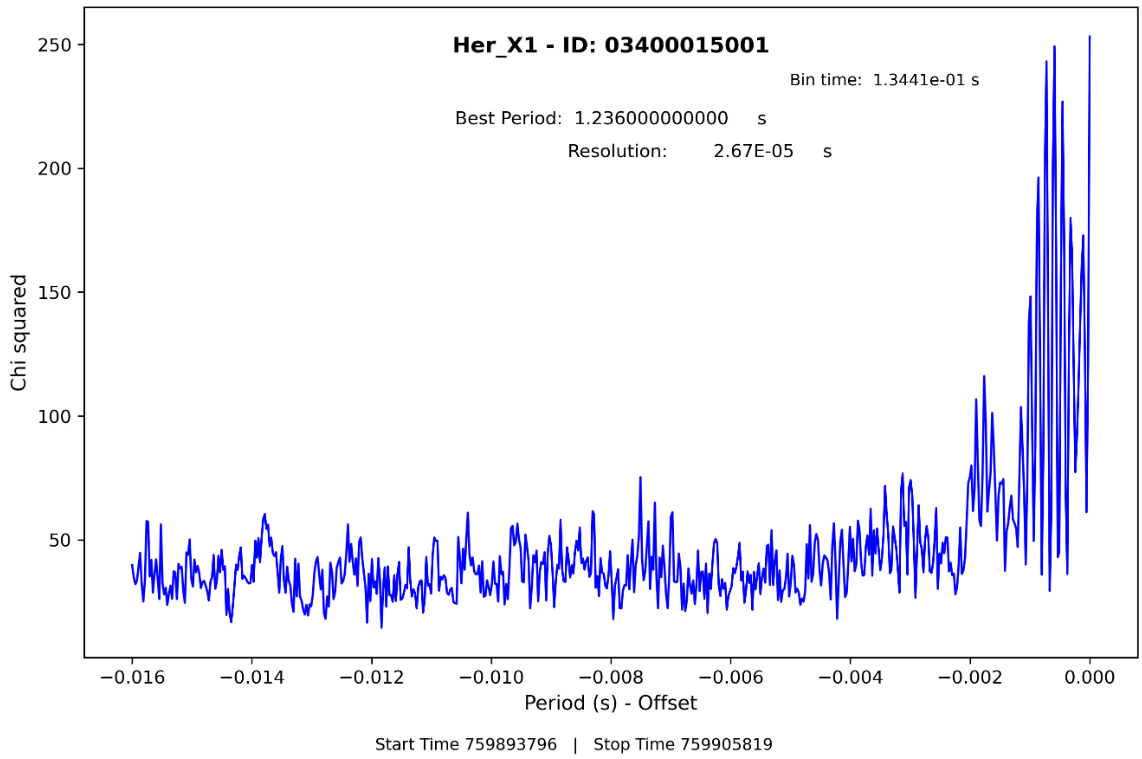


**Figure 9:** Chi-squared Period Search
The results of the efsearch analysis. The best-fit spin period of the pulsar is given by the maximum value of \chi^2 peak. Best Period: 1.236 sec.

## 4.4 PULSE PROFILE EXTRACTION AND EPOCH FOLDING (EFOLD)

The efold task was used to fold pulse characteristics over many phase bins using the optimal spin period obtained from efsearch. The resulting pulse profiles show strong single or multi-peaked patterns characteristic of channeled polar cap emission, together with high signal-to-noise ratios. Phase alignment across sub-intervals allows for clear comparisons between various observational snapshots and verifies rotational stability. We used epoch folding to conduct a period search in a small period interval surrounding the anticipated pulse period (about 1.237 s). In every instance, the integration period was selected to be sufficiently long to provide a pulse profile with adequate statistics (D. Klochkov et al 2009). The shoulder peak vanishes after MJD 58905, while the main peak remains (Yang, W., et al 2026). One of these objects' distinguishing characteristics is the pulse profile (PP), which is calculated by folding the XBP light curve over the spin period, $P_{spin}$ (.D'Aì, A., et al . 2025).

Figure 10 shows the phase-folded pulse profile of Her X-1 obtained from observation ID 03400064001. The structure of the neutron star's profile gives information about the periodicity of the star; the emission of the star x-ray pulsar was clearly recorded as the pulses were binned according to the pulsar's observed period.
The Her X-1 epoch-folded pulse profile for observation ID 03400064002 is also shown in a Figure 11. The continuous rotational modulation recorded at this particular pointing period is reflected in the depicted counts per bin over two complete phase cycles.
The phase-folded pulse profile (eFold Profile) of Her X-1 for observation ID 03400015001 is shown in Figure 12. The source's consistent pulsation properties across the prescribed integration interval are demonstrated by the unique dual-peaked shape.

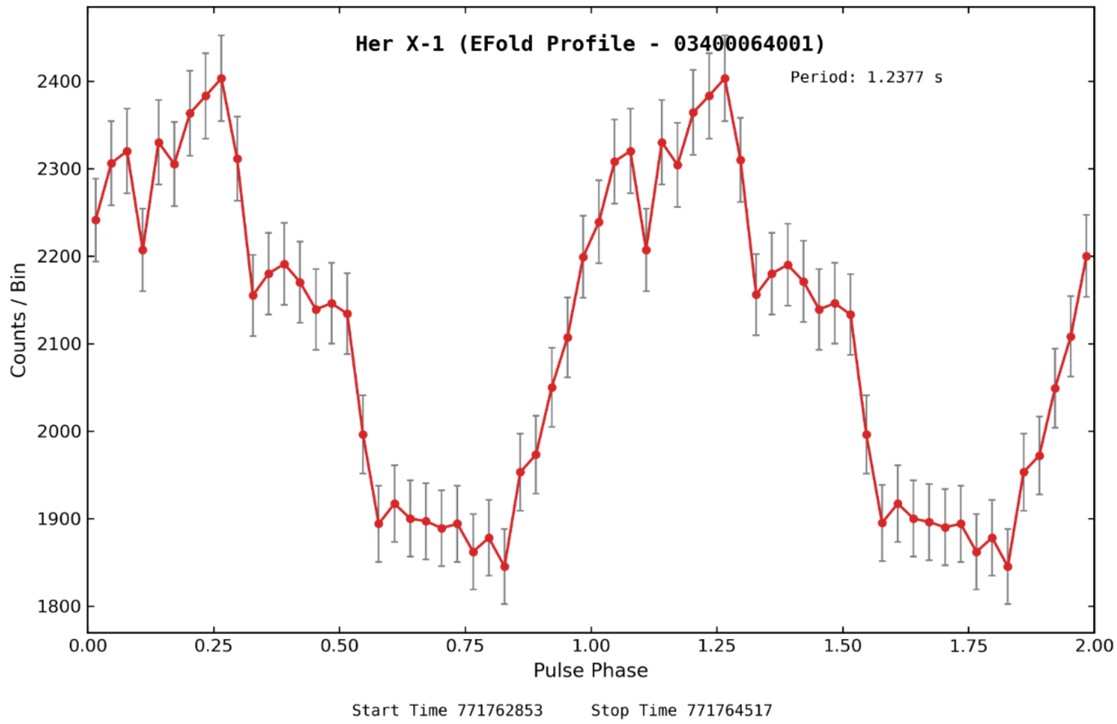


**Figure 10** The Her X-1 epoch folded pulse profile showing counts per bin as purpose of the pulse phase, with a pulse period of approximately 1.237 seconds.

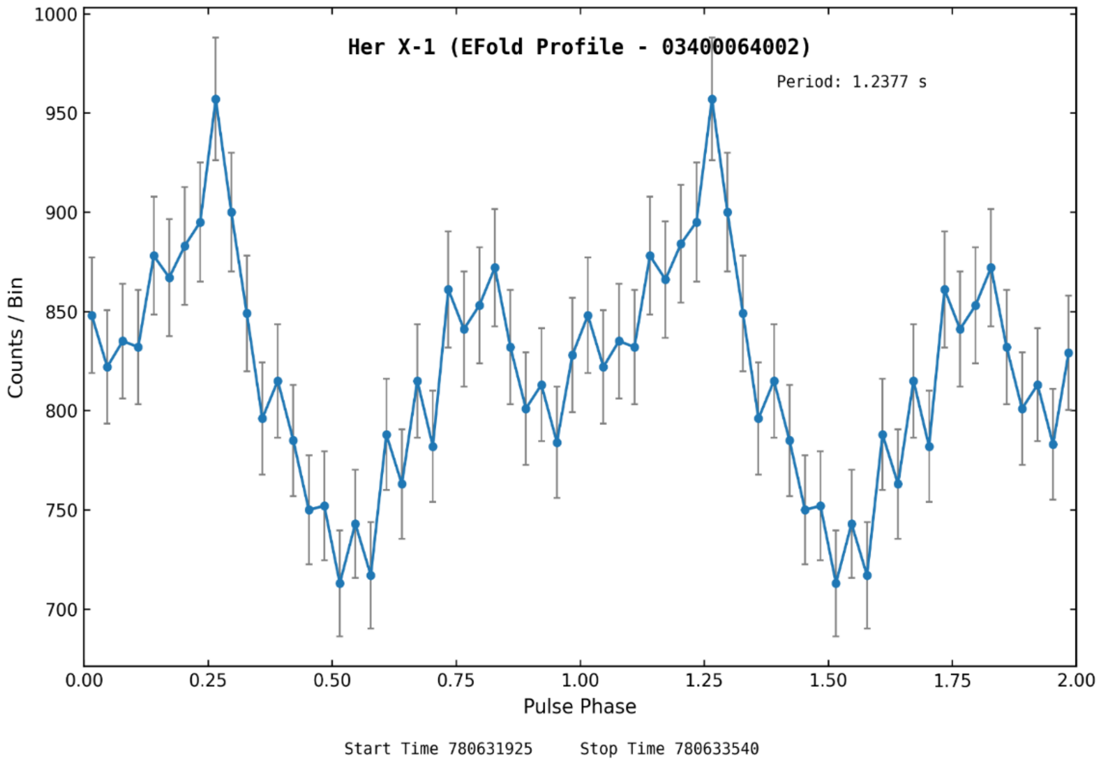


**Figure 11** The Her X-1 epoch folded pulse profile showing counts per bin as purpose of the pulse phase, with a pulse period of approximately 1.2377 seconds.

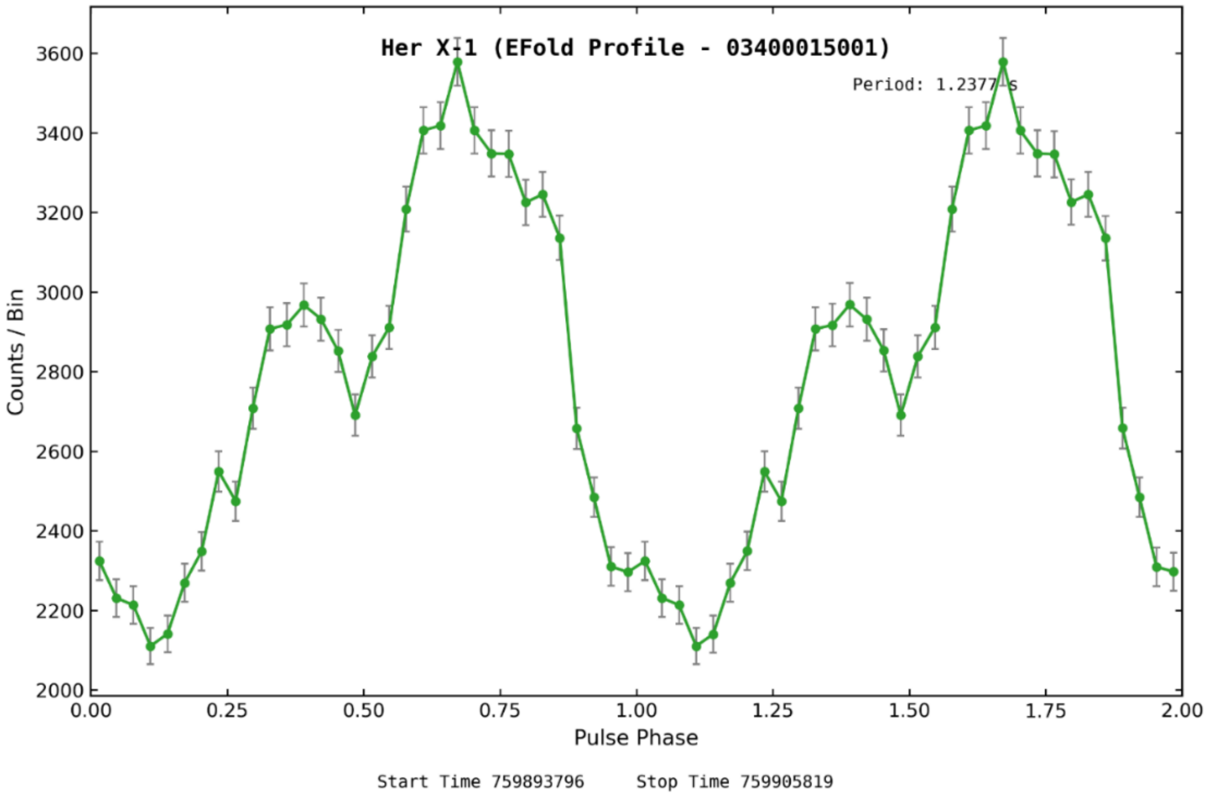


**Figure 12** The Her X-1 epoch folded pulse profile showing counts per bin as purpose of the pulse phase, with a pulse period of approximately 1.2377 seconds.

### 4.5 VARIATIONS IN THE ENERGY-RESOLVED PULSE PROFILE

Pulse patterns were retrieved across discrete, restricted energy bands in order to comprehend the interaction of radiation with the materials surrounding neutron star. Energy-resolved study shows that the pulse shape strongly depends on photon energy. Changes in the beaming geometry, fan-beam vs core-beam emission modes, and energy-dependent scattering optical depths inside the accretion column are reflected in the unique fractional amplitudes and phase shifts of the soft as well as hard energy bands. The Swift satellite's XRT focusing instrument operates in the energy range of

0.2 to 10 keV (Şahiner, Ş., 2013). The photons are divided into three energy bands (total, soft and hard) and the dependence of the change in structure according to the photon's energy and the shape of the pulse are emphasized.

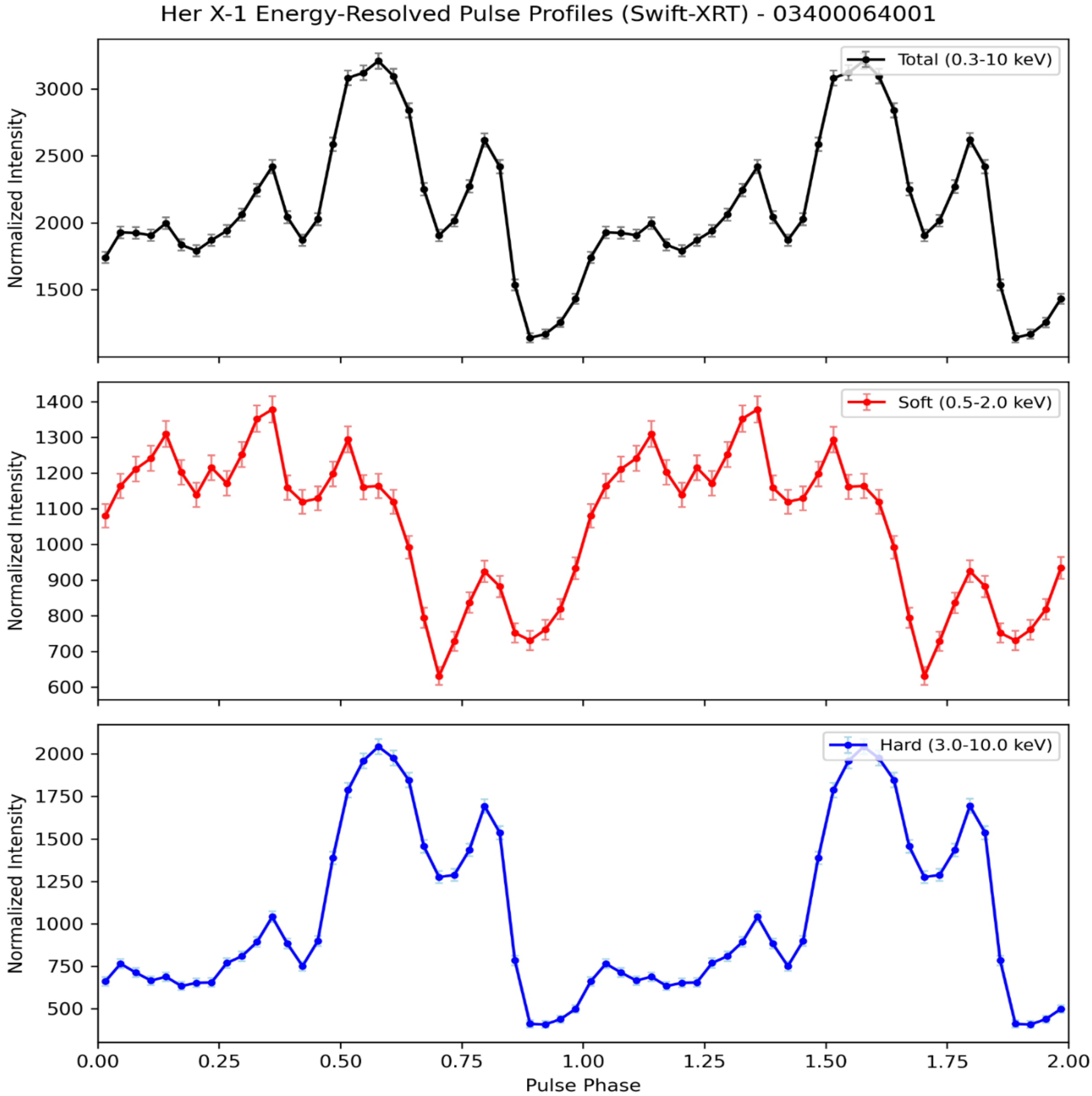


**Figure 13** The energy resolved pulse patterns of Her X-1 are given in the Swift-XRT observation ID 03400064001 in total light, soft energy and hard energy bands. The intensity distribution and pulse shape is shown in this breakdown for different photon energy bands.

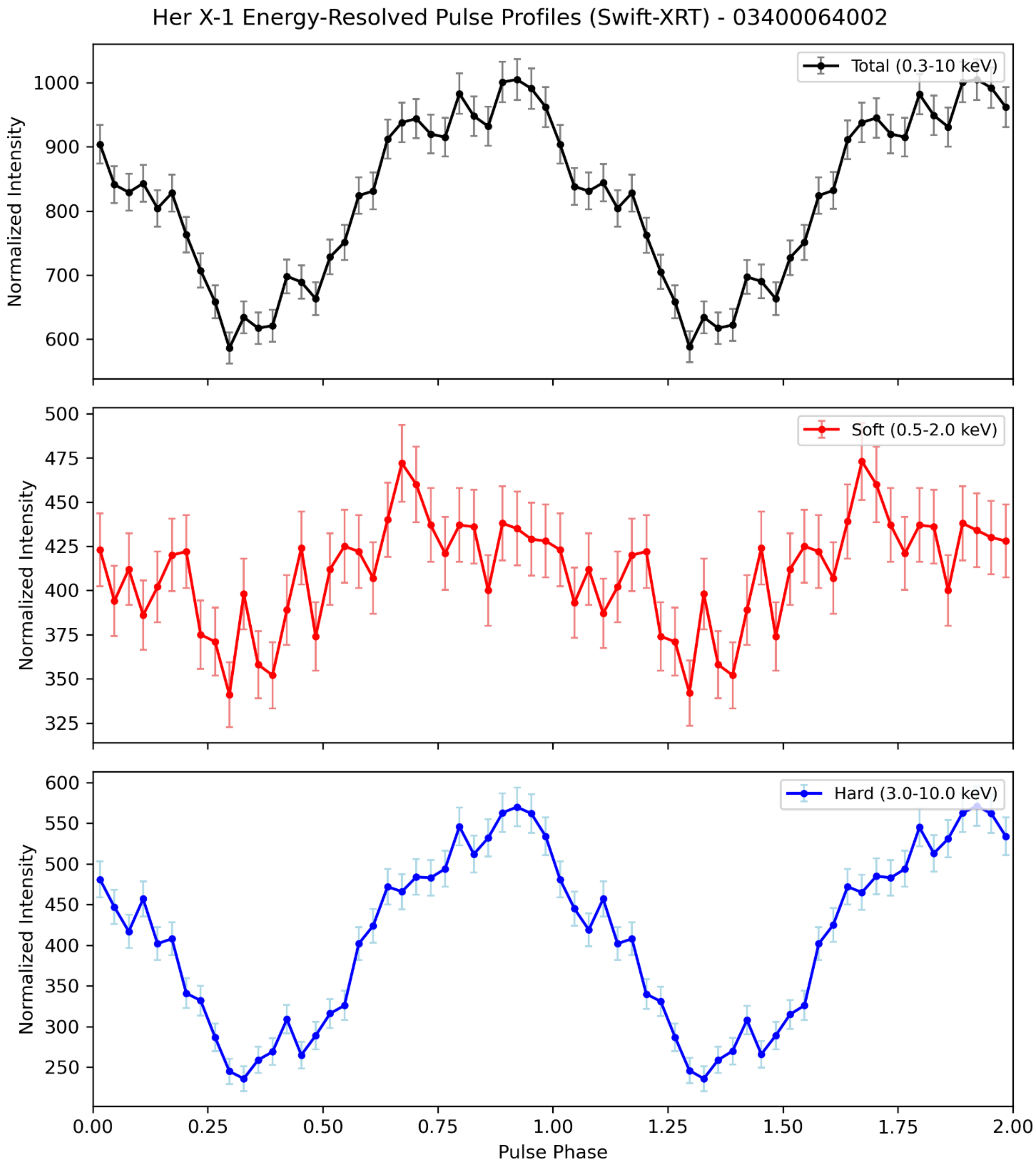


**Figure 14** Energy-resolved pulse profile of Her X-1 (Obs ID: 03400064002) in standard 'spectral windows'. Comparing the trends, it is emphasized that the structure of the pulsed emission in energy during the entire time of observation is noted.

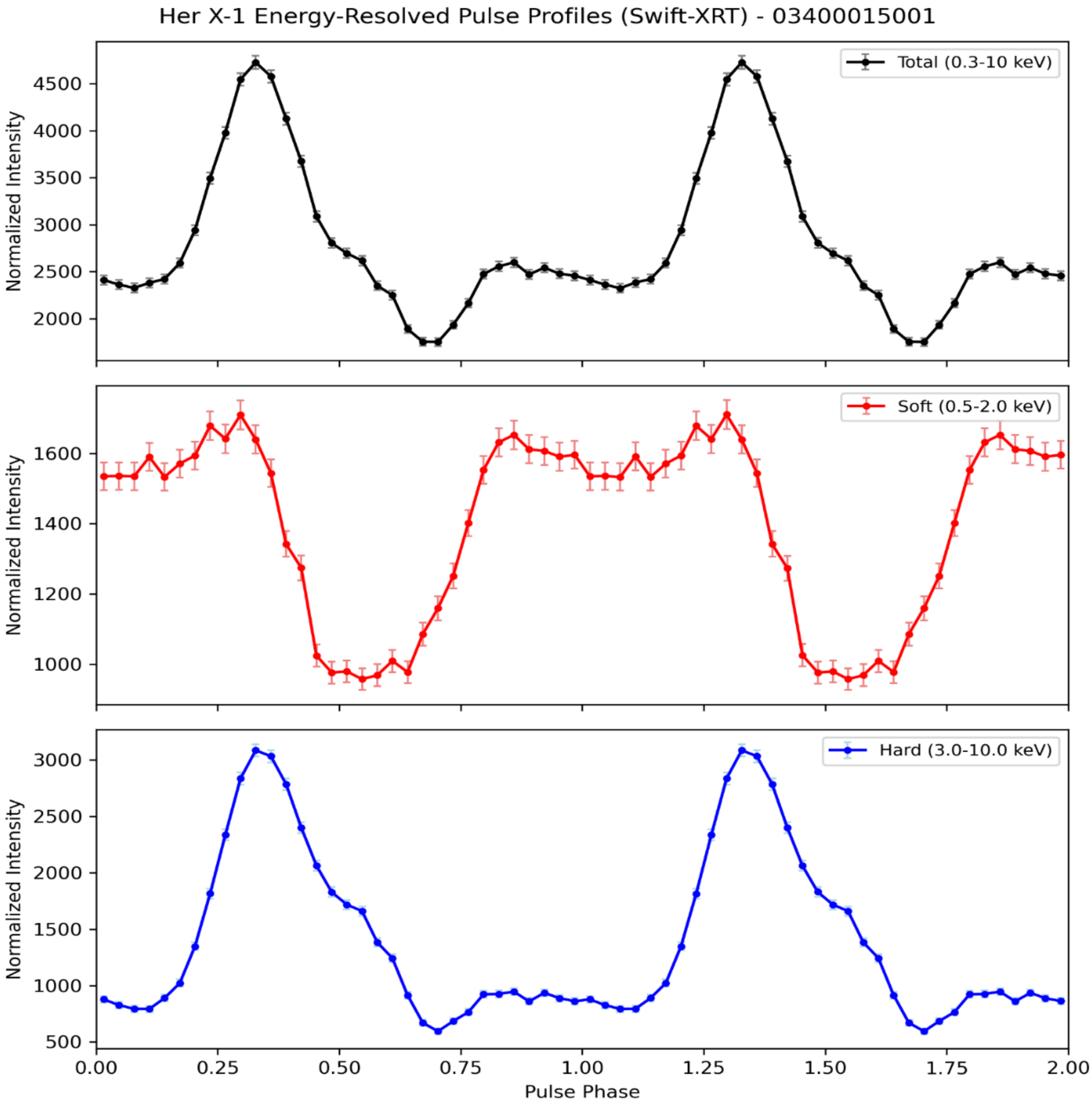


**Figure 15** Generates the resolved pulse patterns for energy emitted by Her X-1 (observation # 03400015001). The number of photons in each of the energy bands in the profiles can be split into energy bands of "hard" energy, "whole" energy and "soft" energy, showing differences in the count profiles which are important to the underlying radiative processes.

## 5. ABSORPTION DYNAMICS AND PHYSICAL DISCUSSION

Here's a summary of the type of pulse patterns and time characteristics observed and their physical implications. The process of Comptonisation in the plasma and the plasma opacities and the dependence of pulse form on the viewpoint in the rotational magnetic poles are considered based on the energy dependence of the pulse form. Moreover, dynamic disparities in the column density of intervening material, such as the precessing accretion disk rim, stellar wind streams, or absorbing structures close to the magnetic foot points, are revealed by the examination of absorption characteristics. This investigation limits the physical mechanisms controlling mass accretion, magnetic field geometry, and radiative transmission in the Her X-1 system during the 2025 epoch by comparing the temporal parameters with theoretical emission models. During the 2015 and 2022 outbursts, SMC X-2 was detected with NuSTAR at the luminosities greater than Eddington perimeter of classical neutron star. It is discovered that the NuSTAR pulse patterns vary on brightness. A doubly peaked profile develops throughout soft to hard X-rays at a brightness of 6.1 × 1038 erg s−1, indicating emission from both poles of the neutron star because the observed peaks are separated by 0.5 phase in the pulse profile (Jaisawal, G. K., et al 2023).

## 6. RESULT AND DISCUSSION

The pulse profiles of Her X-1 generated from Swift/XRT observations reveal a strong dependence on photon energy across the 0.3 to 10.0 keV band. This soft component is generally attributed to thermal emission from the heated polar cap, inner accretion disk rim, or hard X-rays reprocessing by the inner edge of condensation of the precessing accretion disk and the companion star's atmosphere (HZ Her). At advanced energies (2.0 - 10.0 keV), the pulse profiles start to alter and show a distinct asymmetric, multi-peaked morphology sometimes with significant primary and secondary peaks. The energy-dependent evolution is due to the complicated geometry of the accretion column, as well as the fact that the hot electrons of the accretion column are main hard photon sources, thermal Comptonization of soft photons. Direct observation of the emission region enables measurements with very high statistics and a well defined dual-peaked profile in the Main-On state in different phases of the 35 day cycle. These deviations are triggered by the change in the continuum because of the enhanced absorption in an anomalous state or during a transition phase, as an outcome of the precessing and twisting accretion disk. For this reason the results are representative of the special spectroscopic capabilities of Swift/XRT and consistent with previous broad-band observations by other observatories like RXTE and XMM-Newton.

## 7. CONCLUSION

We used archival Swift/XRT observations to give a thorough temporal analysis of the accreting X-ray pulsar Hercules X-1. They are very energy-dependent, with smooth moreover single-peaked pulse profiles in the soft X-ray band (0.3–2keV) and more complicated double-peaked pulse profiles in the harder band (2–10keV) for Her X-1, are the main results of our study. This implies that there are several emission mechanisms present like the direct beamed radiation from the magnetic poles which is Comptonized, thermal reprocessed emission, etc. The time evolution of the pulse profiles in different energy bands and superorbital phases of 35 days also show that the magnetic neutron star accretion flow is time varying, an additional indication being that Swift/XRT data can be used to investigate the physical conditions and emission geometries of magnetic neutron star systems. These observational data are taken specifically for the purpose of targeted observations and have been used to carry out a comprehensive study of the time and energy resolved X-ray spectrum of a time resolved accreting X-ray pulsar, Her X-1. A summary of the main results is as follows: detailed mapping of the light curve and pulse power density spectrum of the pulse, light curves, power density spectra, in multiple bands; description of a number of complex pulse changes with energy measurement; precise measurement of the pulse time. The results stress the significance of energy dependent absorption processes and the dynamic but steady accretion flow. Ultimately, this work expands our understanding of high-energy radiative processes in strongly magnetized neutron star binary systems and paves the way for additional multi-wavelength investigations.

## 8. ACKNOWLEDGMENTS

The authors gratefully acknowledge the use of public data from the Swift/XRT data archive as well as software provided by the HEASARC online service, provided by NASA/GSFC. N.S. expresses sincere gratitude to the Department of Physics, J.R.N. Rajasthan Vidyapeeth (Deemed to be) University, Udaipur, for providing the necessary academic environment and research facilities. We also thank our colleagues for insightful discussions regarding high-energy astrophysical data reduction and timing analysis.

## 9. REFERENCES

1. Fürst, F., Grefenstette, B. W., Staubert, R., Tomsick, J. A., Bachetti, M., Barret, D., ... & Wilms, J. (2013). The smooth cyclotron line in Her X-1 as seen with Nuclear Spectroscopic Telescope Array. *The Astrophysical Journal*, *779*(1), 69.
2. Fürst, F., Grefenstette, B. W., Staubert, R., Tomsick, J. A., Bachetti, M., Barret, D., ... & Zhang10, W. THE SMOOTH CYCLOTRON LINE IN HER X-1 AS SEEN WITH NUSTAR.
3. Klochkov, D., Staubert, R., Postnov, K., Shakura, N., & Santangelo, A. (2009). Continuous monitoring of pulse period variations in Her X-1 using Swift/BAT. *arXiv preprint arXiv:0908.0053*.
4. Godet, O., Beardmore, A. P., Abbey, A. F., Osborne, J. P., Cusumano, G., Pagani, C., ... & Moretti, A. (2009). Modelling the spectral response of the Swift-XRT CCD camera: experience learnt from in-flight calibration. *Astronomy & Astrophysics*, *494*(2), 775-797.
5. Ferrigno, C., Bozzo, E., Falanga, M., Stella, L., Campana, S., Belloni, T., ... & Papitto, A. (2011). INTEGRAL, Swift, and RXTE observations of the 518 Hz accreting transient pulsar Swift J1749. 4− 2807. *Astronomy & Astrophysics*, *525*, A48.
6. Leahy, D., & Wang, Y. (2020). Swift/BAT and RXTE/ASM Observations of the 35 day X-Ray Cycle of Hercules X-1. *The Astrophysical Journal*, *902*(2), 146.
7. Xiao, G. C., Staubert, R., Ji, L., Ge, M. Y., Liu, Q. Z., Qu, J. L., ... & Yang, Z. X. (2024). Insight-HXMT Views Her X-1: Probing the Dependence of the Cyclotron Line Energy on Flux and Time. *The Astrophysical Journal*, *960*(1), 57.
8. Şahiner, Ş., İnam, S. Ç., Serim, M. M., & Baykal, A. L. T. A. N. (2013). RXTE and Swift observations of SWIFT J1729. 9− 3437. *Monthly Notices of the Royal Astronomical Society*, *434*(4), 2772-2778.

9. Jayasurya, K. M., Upadhyay, A., & Rana, V. (2026). Discovery of a Candidate 2 keV Cyclotron Resonance Scattering Feature in the HLX NGC 3583 X-1. *arXiv preprint arXiv:2606.08598*.
10. Chou, Y. (2026). Superorbital Phase Evolution and a Soft–Hard X-Ray Phase Shift in LMC X-4. *The Astrophysical Journal*, *1000*(1), 23.
11. Coley, J. B., Corbet, R. H., Fürst, F., Huxtable, G., Krimm, H. A., Pearlman, A. B., & Pottschmidt, K. (2019). A Study of the 20 day Superorbital Modulation in the High-mass X-Ray Binary IGR J16493-4348. *The Astrophysical Journal*, *879*(1), 34.
12. Jaisawal, G. K., Vasilopoulos, G., Naik, S., Maitra, C., Malacaria, C., Chhotaray, B., ... & Sanna, A. (2023). On the cyclotron absorption line and evidence of the spectral transition in SMC X-2 during 2022 giant outburst. *Monthly Notices of the Royal Astronomical Society*, *521*(3), 3951-3961.
13. Brightman, M., Bachetti, M., Earnshaw, H., Fürst, F., Heida, M., Israel, G. L., ... & Walton, D. J. (2022). Evolution of the Spin, Spectrum and Superorbital Period of the Ultraluminous X-Ray Pulsar M51 ULX7. *The Astrophysical Journal*, *925*(1), 18.
14. Kuiper, L., Hermsen, W., & Dekker, A. (2018). The Fermi-LAT detection of magnetar-like pulsar PSR J1846−0258 at high-energy gamma-rays. *Monthly Notices of the Royal Astronomical Society*, *475*(1), 1238-1250.
15. Ferrigno, C., D'Aì, A., & Ambrosi, E. (2023). Energy-resolved pulse profiles of accreting pulsars: Diagnostic tools for spectral features. *Astronomy & Astrophysics*, *677*, A103.
16. Zhao, Q. C., Li, H. C., Tao, L., Feng, H., Zhang, S. N., Walter, R., ... & Zhao, K. (2024). Polarization perspectives on Hercules X-1: Further constraining the geometry. *Monthly Notices of the Royal Astronomical Society*, *531*(4), 3935-3949.
17. Staubert, R., Klochkov, D., Wilms, J., Postnov, K., Shakura, N. I., Rothschild, R. E., ... & Harrison, F. A. (2014). Long-term change in the cyclotron line energy in Hercules X-1. *Astronomy & Astrophysics*, *572*, A119.
18. Yang, W., Wang, W., & Zhou, Q. (2026). Measurement of the Orbital Parameters, Spin, and Spectral Evolution during the Main High State of Her X-1 with Insight-HXMT. *The Astrophysical Journal*, *1002*(1), 43.
19. D'Aì, A., Maniadakis, D. K., Ferrigno, C., Ambrosi, E., Sokolova-Lapa, E., Cusumano, G., ... & Rodríguez-Castillo, G. A. (2025). Energy-resolved pulse profile changes in V 0332+ 53: Indications of wings in the cyclotron absorption line profile. *Astronomy & Astrophysics*, *694*, A316.
20. Fuerst, F., Grefenstette, B. W., Staubert, R., Tomsick, J. A., Bachetti, M., Barret, D., ... & Zhang, W. (2013). The smooth cyclotron line in Her X-1 as seen with NuSTAR. *arXiv preprint arXiv:1309.5361*.
21. Ferrigno, C., Bozzo, E., & Romano, P. (2022). XMM-Newton and Swift observations of supergiant high mass X-ray binaries. *Astronomy & Astrophysics*, *664*, A99.
22. Salganik, A., Tsygankov, S. S., Doroshenko, V., Molkov, S. V., Lutovinov, A. A., Mushtukov, A. A., & Poutanen, J. (2023). RX J0440. 9+ 4431: another supercritical X-ray pulsar. *Monthly Notices of the Royal Astronomical Society*, *524*(4), 5213-5224.
23. Pasham, D. R., & Strohmayer, T. E. (2013). Evidence for Quasi-periodic X-Ray Dips from an Ultraluminous X-Ray Source: Implications for the Binary Motion. *The Astrophysical Journal*, *764*(1), 93.
24. Marcu-Cheatham, D. M., Pottschmidt, K., Kühnel, M., Müller, S., Falkner, S., Caballero, I., ... & Wilms, J. (2015). The Transient Accreting X-Ray Pulsar XTE J1946+ 274: Stability of X-Ray Properties at Low Flux and Updated Orbital Solution. *The Astrophysical Journal*, *815*(1), 44.
25. Paul, B., & Naik, S. (2011). Transient high mass X-ray binaries. *arXiv preprint arXiv:1110.4446*.
26. Esposito, P., Israel, G. L., Sidoli, L., Tiengo, A., Campana, S., & Moretti, A. (2014). The X-ray emission of the high-mass X-ray binary IGR J17200− 3116. *Monthly Notices of the Royal Astronomical Society*, *441*(2), 1126-1133.